9-2019

Multiscale Modeling of Superior Cavopulmonary Circulation: Hemi-Fontan and Bidirectional Glenn Are Equivalent

Ethan Kung

Chiara Corsini

Alison Marsden

Irene Vignon-Clemente

Giancarlo Pennati

See next page for additional authors

Authors

Ethan Kung, Chiara Corsini, Alison Marsden, Irene Vignon-Clemente, Giancarlo Pennati, Richard Figliola, and Tain-Yen Hsia

Seminars in Thoracic and Cardiovascular Surgery
DOI: https://doi.org/10.1053/j.semtcvs.2019.09.007

Full Title: Multiscale Modeling of Superior Cavopulmonary Circulation: Hemi-Fontan And Bidirectional Glenn Are Equivalent

Authors: Ethan Kung[1]; Chiara Corsini[2]; Alison Marsden[3]; Irene Vignon-Clementel[4]; Giancarlo Pennati[2]; Richard Figliola[1,*], and Tain-Yen Hsia[5,*]; for the Modeling of Congenital Hearts Alliance (MOCHA)+ Investigators

Affiliations:

1. Clemson University, Clemson, SC, USA,
2. Politecnico di Milano, Milan, Italy
3. Stanford University, Stanford, CA
4. National Institute for Research in Computer Science and Automation (INRIA), Paris, France
5. Yale New Haven Children's Hospital, New Haven, CT

§ co-first authors
* co-senior authors

MOCHA Investigators: Andrew Taylor, Sachin Khambadkone, Silvia Schievano, and Marc de Leval (Institute of Cardiovascular Sciences, London, UK); Edward Bove, and Adam Dorfman, (University of Michigan, Ann Arbor, MI); G. Hamilton Baker and Anthony Hlavacek (Medical University of South Carolina, Charleston, SC); Francesco Migliavacca, Giancarlo Pennati, and Gabriele Dubini (Politecnico di Milano, Milan, Italy); Alison Marsden, (Stanford University, CA); Irene Vignon-Clementel (National Institute of Research in Informatics and Automation, Paris, France); Richard Figliola and John McGregor (Clemson University, Clemson, SC); Tain-Yen Hsia (Yale University, New Haven, CT)

Total word count: 5924

Funding and Conflicts of Interest:
This work received funding support from Leducq Foundation (France), National Institute of Health Research (UK), Burroughs Wellcome Fund (UK), American Heart Association (US), National Science Foundation (US) and British Heart Foundation (UK). All authors have nothing to disclose regarding possible conflicts of interest.

Corresponding Author:

T-Y Hsia, MD
Pediatric Cardiac Surgery
Yale New Haven Children's Hospital
LCCI 301, 330 Cedar Street
New Haven, CT, USA
Telephone: 1 (203) 737-1298
Email: tain-yen.hsia@yale.edu

Glossary

Abbreviations

$art_{sat\text{-}pre}$	preoperative arterial oxygen saturation
$art_{sat\text{-}post}$	post-operative arterial oxygen saturation
bG	bi-directional Glenn
BSA	body surface area
CFD	computational fluid dynamics
CI	cardiac index
CMR	cardiac magnetic resonance imaging
CS	central shunt
GA	general anaesthetic
Hb	hemoglobin
hF	hemi-Fontan
HLHS	hypoplastic left heart syndrome
IVC	inferior vena cava
LPA	left pulmonary artery
LPN	lumped parameter network
$maxO_2cap$	maximum oxygen capacity
mBTS	modified Blalock-Taussig shunt
O_2del	systemic oxygen delivery
O_2cons	oxygen consumption
PA	pulmonary arteries
PAP	pulmonary artery pressure
PVR	pulmonary vascular resistance
$PV_{sat\text{-}pre}$	pre-operative pulmonary venous oxygen saturation
Q_p	pulmonary blood flow rate
$Q_{p\text{-}pre}$	pre-operative pulmonary blood flow rate
Q_s	systemic blood flow rate
SVC	superior vena cava
SCPC	superior cavopulmonary connection/circulation
TPG	transpulmonary gradient

Abstract

Objective: Superior cavopulmonary circulation (SCPC) can be achieved by either the Hemi-Fontan (hF) or Bidirectional Glenn (bG) connection. Debate remains as to which results in best hemodynamic results. Adopting patient-specific multiscale computational modeling, we examined both the local dynamics and global physiology to determine if surgical choice can lead to different hemodynamic outcomes.

Methods: Six patients (age: 3-6 months) underwent cardiac magnetic resonance imaging and catheterization prior to SCPC surgery. For each patient: 1) a finite 3-dimensional (3D) volume model of the *preoperative* anatomy were constructed to include detailed definition of the distal branch pulmonary arteries, 2) virtual hF and bG operations were performed to create *two* SCPC 3D models, and 3) a specific lumped network representing each patient's entire cardiovascular circulation was developed from clinical data. Using a previously validated multiscale algorithm that couples the 3D models with lumped network, both local flow dynamics, i.e. power loss, and global systemic physiology can be quantified. In two patients whose preoperative imaging demonstrated significant left pulmonary artery (LPA) stenosis, we performed virtual pulmonary arterioplasty to assess its effect.

Results: In one patient, the hF model showed higher power loss (107%) than the bG, while in 3 the power losses were higher in the bG models (18 to 35%). In the remaining two patients, the power loss differences were minor. Despite these variations, for all patients, there were no significant differences between the hF and bG models in hemodynamic or physiologic outcomes, including cardiac output, superior vena cava pressure, right-left pulmonary flow distribution, and systemic oxygen delivery. In the two patients with LPA stenosis, arterioplasty led to better LPA flow (5-8%) while halving the power loss, but without important improvements in SVC pressure or cardiac output.

Conclusion: Despite power loss differences, both hF and bG result in similar SCPC hemodynamics and physiology outcome. This suggests that for SCPC, the pre-existing patient-specific physiology and condition, such as pulmonary vascular resistance, are

more deterministic in the hemodynamic performance than the type of surgical palliation. Multiscale modeling can be a decision assist tool to assess whether an extensive LPA reconstruction is needed at the time of SCPC for LPA stenosis.

(Word count = 359)

Perspective Statement

Whether hemi-Fontan or bidirectional Glenn achieves a better superior cavopulmonary circulation remains debatable. Mathematical modelling incorporating both the 3D anatomic detail and systemic physiology can elucidated effects of surgery in a patient specific manner. We applied state of the art computational methods to demonstrate that either palliation led to equivalent hemodynamic outcomes, despite differences in local power loss.

Word count: 58 (379 characters)

Central Message

Advanced modeling simulation showed that the hemi-Fontan and bidirectional Glenn achieves early equivalent superior cavopulmonary circulation hemodynamics and physiology.

Word-count: 18 (163 characters)

Introduction

Superior cavopulmonary connection (SCPC) is a transitional circulation that allows for volume off-loading of the single ventricle while providing a stable source of pulmonary blood flow that can grow with the patient prior to completing single ventricle palliation with a Fontan procedure. Pioneered by William Glenn at Yale in the 1960's, the classic unidirectional Glenn anastomosis has been replaced by either the bidirectional Glenn (bG) or the hemi-Fontan (hF) procedures. While a hF facilitates Fontan completion with a lateral tunnel total cavopulmonary connection (TCPC), bG permits creation of an extracardiac TCPC without the need for cardioplegic cardiac arrest. Nonetheless, the choice between the adaptation of either the bG or hF to achieve SCPC remains primarily based on surgeon or institutional preferences. Whereas no direct, randomized comparative study has been performed to demonstrate outcome differences between the two SCPC procedures, the question regarding whether one is superior than the other remains unanswered with two opposing modeling studies highlighting superiority of one versus the other.[1,2]

While methodologically accurate, both of the previous computational modeling investigations focused solely on the *local* flow dynamics, i.e. the flow and pressures *at* the bG or hF connection. And in so doing, both studies relied on local flow dynamic variables, such as power loss and flow split between the branch pulmonary arteries, to assess performance differences between the bG and hF circulations. However, because the SCPC is just one segment of the global cardiovascular system that is composed of a closed circulatory loop, isolated SCPC modeling with open ended boundary conditions cannot reveal the influence of either the bG or hF on the overall systemic physiology such as SVC pressure, cardiac output, and systemic oxygen delivery.

Multi-scale modeling combines the strengths of 3D computational fluid dynamics (CFD) with 0-D lumped parameter network to allow comprehensive assessment of hemodynamic effects of the local surgical domain and the global impact on the systemic physiology. Over the last decade, we have used these validated multi-scale models to evaluate a

variety of clinically significant issues and concepts in patients with single ventricle physiology, such as the hybrid procedure for HLHS, branch pulmonary artery stenosis, residual coarctation, systemic-to-pulmonary shunts, exercise physiology, cardiac biomechanics, and alternative initial palliation, and virtual surgery. [3-6]

In this study, we conducted an intensive mathematical modeling investigation using clinical data obtained from a cohort of six patients with single ventricle hearts undergoing SCPC procedure to uncover whether the choice between bG and hF procedures leads to hemodynamic and physiological differences. In addition to the employment of the multi-scale modeling scheme with a closed-loop cardiovascular circulation, other novel concepts in this study include: 1) adaptation of *patient-specific* anatomy (with detailed distal branch pulmonary arteries) and physiologic parameters into the models, 2) performing virtual bG and hF procedures based on preoperative magnetic resonance imaging, 3) examining the effects of relieving *patient-specific* discrete left pulmonary artery (LPA) stenosis at the time of SCPC procedure, and 4) quantifying both hemodynamic and physiologic variables in the context of SCPC.

Methods

Patient Selection and Clinical Data

Six patients (age: 3-6 month, BSA: 0.26-0.34 m^2) with single ventricle cardiac defects were enrolled prior to their pre-operative clinical investigations prior to their SCPC procedure. Patients A, E, and F were recruited at the University of Michigan, B and D at the Medical University of South Carolina, and patient C at Great Ormond Street Hospital for Children (GOSH). Institutional review board study approval was obtained for each clinical site and informed consent for the use of clinical data was gained from the participants' legal guardians. The pre-operative clinical details of the six patients are reported in Table 1. Four patients had hypoplastic left heart syndrome (HLHS) and two had a hypoplastic right ventricle. At the stage 1 surgery, patient A received a 3.5mm right modified Blalock-Taussig shunt (mBTS), patients B,C,E,F underwent Norwood procedure with 3.5mm right mBTS, and patient D had a 4mm mBTS with left pulmonary arterioplasty.

All patient underwent pre-operative cardiac magnetic resonance imaging (CMR), cardiac catheterization and echocardiography prior to surgery. Depending on institutional preferences, CMR was either performed immediately prior to surgery under the same general anesthesia (GA), on the day of cardiac catheterization under the same GA with transfer between imaging suites, or in a hybrid CMR catheterization imaging suite. CMR was performed on 1.5T scanners (Philips Intera Achieva, Best, Netherlands; Siemens Avanto, Siemens Medical Solutions, Erlangen, Germany). Contrast enhanced CMR angiography was performed to obtain three-dimensional (3D) anatomical imaging with a routine clinical sequence using 0.2mmol/kg of intravenous gadoteridol (Prohance; Bracco Diagnostics, Princeton, NJ). Free-breathing, electrocardiogram-gated velocity-encoded phase contrast imaging sequences were used to acquire flow measurements in the ascending and descending aorta, pulmonary arteries and veins, and inferior (IVC) and superior vena cavae (SVC).

Cardiac catheterization followed a routine clinical protocol under GA or sedation in a bi-plane fluoroscopy suite (Siemens Medical Solutions USA, Inc. Pennsylvania). A fluid-filled catheter system was used to acquire pressure traces and hemodynamic measurements in the ascending and descending aorta, systemic atrium, and single ventricle. Pulmonary artery pressure (PAP) was either a direct measurement or an estimate from pulmonary venous wedge pressure. In patients C, E, and F, PAP was acquired on the left side, with no clinical evidence suggestive of a stenosis or cause for discrepancy between the two pulmonary arteries (PA). In patients A, B, and D, PAPs were acquired on the left and right sides. Patient B also had left pulmonary artery stenosis (PAS), and patient D had left PAS with a 3mmHg pressure difference between the two pulmonary arteries. Only in patient D did the clinical team felt a left pulmonary arterioplasty was indicated. Pre-operative echocardiography was performed under GA or sedation. Pulsed wave Doppler traces were acquired in the aorta, SVC, IVC and branch PAs.

All clinical data processing occurred at one core laboratory (GOSH). A representation of the patients' pre-operative physiology was constructed from CMR flows and invasive mean pressure measurements. The resulting parameters presented in Table 2 were used to tune the multiscale models as described below. Flow measurements were calculated using an in-house plug-in for OsiriX open-source software (OsiriX Foundation, Geneva, Switzerland). These are reported indexed to BSA to aid comparison between patients.

Three-dimensional (3D) models and virtual surgery

3D models of each patients' stage 1 anatomy were reconstructed from the CMR angiographic sequences using commercially available software (Mimics, Materialise NV, Leuven, Belgium). In Figure 1, we illustrate the reconstruction process using Patient B as an example, while Figure 2 depicts the stage 1 and stage 2 reconstructions for the six patients studied. Referring to Figure 1, a region of interest was selected within the relevant area of surgical anatomy. A 3D geometrical model was constructed through a process of region-growing and segmentation.[7,8] The pre-operative 3D model for each patient included the mBTS and PAs extended to the furthest branch level visible for reconstruction

(Figure 1, stage 1). The location of the SVC and atrium was noted for construction of the stage 2 virtual surgery. To this end, the stage 1 geometry was manipulated virtually, removing the mBTS and inserting the reconstructed SVC in its stead, merging the volumes with a Boolean operation (Figure 1, stage 2). In the case of hF, a portion of the atrium was reconstructed from the original CMR dataset and similarly merged in the 3D domain, again after removal of the mBTS. In both cases, where appropriate, a pulmonary arterioplasty model was generated by virtually enlarging the caliber of the narrowed PA. Prior to use for stage 2 simulations, the realistic nature of all virtual surgery models shown in Figure 2 was verified by the surgeons (EB, TYH) involved in the study.

Multiscale Simulation and Analysis

Multi-scale models were developed and tuned for each patient based on the patient-specific anatomical and clinical data (Table 2). According to our previous work,[3,4] we constructed a 0D LPN to model the circulatory system outside of the surgical region, which was coupled directly to the inflow and outflow passages of the 3D model of the surgical site. Briefly, the closed-loop LPN includes sections that describe the heart, upper and lower body vasculatures, pulmonary vasculature, and vascular beds in several abdominal organs. The contraction and filling of each heart chamber is described via a passive and active pressure-volume curve and an activation function. [3,4] This allows the simulation to capture effects of preload on cardiac output due to the Frank-Starling mechanism. The influence of respiration was neglected for this study.

Each patient was modeled at the age and body surface area (BSA) at the time of their CMR scan since both 3D and flow information is acquired at this time-point. As described in our prior work, most elements of the LPN were tuned initially using reference values (that were scaled by allometric equations based on each patient's particular BSA and then further adjusted for each patient based on available clinical data. [9-12] The LPN parameters in the pulmonary vasculature were automatically estimated based on multiscale preoperative simulations to match the relevant clinical measurements.[13] We divided the pulmonary vasculature into several parts to be represented as lumped components.

These parts include the large arteries, smaller arteries, capillaries, and veins; Next, empirical laws determined the distribution of the equivalent resistance and capacitance over the arterial or venous sides. [14-16] Windkessel models were generated from the Womersley-based impedance of each pulmonary branch,[17,18] therefore the proximal to distal pulmonary artery resistance ratio is different for each branch. Combining all of these relations provided a unique set of LPN parameters for each pulmonary branch based on its total resistance.

Multi-scale simulations of the post-operative scenarios were conducted according to previously validated techniques. [7, 12, 19, 20] Briefly, this involves discretizing the 3D virtual surgery geometries into isotropic finite-element meshes with maximum edge size of 0.03 cm (MESHSIM, Simmetrix Inc., New York) and coupling the 3D Navier-Stokes equations to the 0D LPN using Neumann boundary conditions, implicit coupling, and outflow stabilization.[21] Flow and pressure in the 3D and LPN domain were solved using a custom incompressible finite element Navier-Stokes solver (Simvascular, www.simtk.org), and a 4^{th} order Runge-Kutta algorithm, respectively. Simulation time step size was 1 ms and 1 μs for the 3D and LPN domain, respectively. Flow and pressure coupling between domains occurs at every 3D time step. Each simulation included 12 cardiac cycles where the last cycle data, by which periodicity had been achieved, was used in the final results analysis.

Power loss was calculated from the simulation results according to our previous publication.[4] To summarize, the surgical junction power loss was obtained from the 3D data by integrating the sum of inlet and outlet face energy fluxes, which accounts for both the potential and kinetic energy. The power loss across a vascular bed was obtained from the 0D data by multiplying the pressure drop and the total flow across the vascular bed.

Post-operative predictions of systemic oxygen delivery, and arterial and venous saturations were calculated using a combination of pre-operative clinical measurements and post-operative predictions of flow. We assumed: 1) the pre-operative estimates of maximum oxygen capacity and oxygen consumption remained the same immediately

following surgery; 2) pulmonary venous saturations remain the same immediately post-operatively; and 3) the relative upper and lower body oxygen consumption after surgery is directly proportional to flow. The maximum oxygen carrying capacity of blood *maxO_2cap* (mlO_2/100ml) was estimated as

$$\max O_2 cap = Hb_{pre} \times 1.34 \quad (1)$$

where Hb_{pre} is pre-operative hemoglobin in g/dL and 1.34 represents Hüfner's constant (a directly measured estimate of the maximum oxygen carrying capacity of blood equal to 1.34ml O2/g of hemoglobin). The oxygen consumption *O_2cons* (mlO_2/min/m^2) was estimated as

$$O_2 cons = Q_{p-pre} \times \frac{PV_{sat-pre} - art_{sat-pre}}{100} \times \max O_2 cap \times 10 / BSA \quad (2)$$

where $Q_{p\text{-}pre}$ is the pre-operative measured pulmonary flow (L/min), $PV_{sat\text{-}pre}$ is the measured pre-operative pulmonary venous oxygen saturations (%), $art_{sat\text{-}pre}$ is the measured arterial oxygen saturations (%), and BSA is body surface area (m^2). The post-operative estimated systemic oxygen delivery *O_2del* (mlO_2/min/m$_2$) was calculated as

$$O_2 del = \frac{(Q_s \times \frac{PV_{sat-pre}}{100} \times \max O_2 cap \times 10) - \frac{(\alpha_{LB} \times O_2 cons \times BSA)}{Qp}}{BSA} \quad (3)$$

where Q_s is systemic flow (L/min) calculated from the post-operative simulation, α_{LB} is the proportion of Q_s to the lower body based on post-operative simulation results, and Q_p is the post-operative pulmonary flow (L/min) from simulation results. The post-operative arterial oxygen saturation $art_{sat\text{-}post}$ (%) was estimated as

$$art_{sat-post} = \frac{O_2 del}{Qs} \times \frac{BSA}{\max O_2 cap \times 10} \quad (4)$$

Results

There were significant differences in local flow patterns and pressure distributions between the two surgical options. Using the results for patient B as an example (Figure 3), the bG geometry typically reveals a flow jet of blood from the SVC that impinges on the bottom of the PA wall at the anastomosis where it divides to the branches (Figure 3, A and C). However, in the hF geometry there is slight vortex of blood as the incoming SVC flow glides along the atrial wall (Figure 3, B and D). In the cases where an LPA stenosis is present (Figure 3, A and B), there is also a flow jet following and a nominal 1mmHg pressure loss across the stenosis. The pressure and flow patterns predicted here were consistent with those of a previous study on patients at the same stage but right before the Fontan surgery.[18]

The local power loss in the surgical SCPC junction (Table 3, 3D power loss) varied considerably between bG and hF models. In four patients, hF showed a notably higher power loss (18 to 107%) than bG ,which was consistent with the differences in flow fields and pressures between these differing surgical options. In two patients, power losses were essentially equivalent (< 7% difference) between options. In comparing the 3D power loss with the total power loss across the entire pulmonary vascular bed (Table 3), the amount of power loss occurring within the SCPC junction is only 1 to 16% of that across the entire pulmonary circulation. The magnitudes of these power losses are compared directly in Figure 4. Much larger differences in the total pulmonary power loss exist between patients with different pulmonary vascular resistances (PVR) than between the different surgical options of the same patient.

As a consequence, the post-operative SCPC simulation results revealed similar physiologic outcomes between the various surgical options for each patient (Table 3). The bG and hF surgical models had small differences in transpulmonary gradient (TPG) and SVC pressure (P_{SVC}) (up to 5% and 2%, respectively), and negligible differences in cardiac index (CI) (<1%) with nearly identical pulmonary to systemic flow splits. Oxygen delivery (Table 3) closely followed cardiac index for each patient, and both oxygen delivery and

oxygen saturations were insensitive to the surgical option for a specific patient.

The power losses in models with left PAS were found to be more than two times higher (217-248%) than that in models where the left PAS was relieved by virtual arterioplasty. While the relief of PAS led to slightly better LPA flow (5-8%) in both patients, there was no important improvement in SVC pressure or cardiac output compared to models where the left PAS was left intact.

Discussion

In 1996, Marc de Leval and his collaborators in Milan, Italy reported the first instance where computational fluid dynamics (CFD), a relatively new engineering field, was applied to the evaluation of a reconstructive cardiac procedure.[24] While the mathematics were sophisticated and investigation revealed interesting flow dynamic insights in the TCPC, the problem facing the investigators was how to translate the mathematical information to the surgical community. They needed a parameter or variable that a congenital cardiac surgeon can appreciate its value and correlate with clinical significance. Since the ability of CFD at that time only allowed for modeling an isolated surgical domain, i.e. the cavopulmonary connections, their models required compulsory open-ended inlets and outlets with rigid, prescribed boundary conditions. And in such an open-loop circulatory model, only the local pressure and flow conditions can be quantified, leaving any interaction with the rest of the global, systemic circulation unanswered. Therefore, as a way to quantify the 'performance' of a cavopulmonary connection, the concept of power loss was introduced to describe the *extraction* of fluid dynamic power, or energy, as blood traversed from the inlets (vena cava) to the outlets (branch pulmonary arteries). Less power loss in a cavopulmonary circulation, the better. And power loss became the goal post for which future modeling investigations of the cavopulmonary circulation would be based on. [1,2,18,22]

In this study, where a closed loop circulatory model allowed for interaction between the SCPC and the rest of the cardiovascular system, our *patient-specific* multi-scale simulations showed that differences in power loss between a hF and bG SCPC, even when greater than two-fold, resulted in negligible effect on clinically relevant parameters such as cardiac index, SVC pressure, and systemic oxygen delivery. Therefore, either hF or bG, as the procedure of choice for SCPC, would achieve similar hemodynamic and physiologic results. This is unlikely to be a controversial finding, as most surgeons would agree that outcomes after either procedure have been viewed to be similar. Nonetheless, by employing the state of art multi-scale modeling with patient-specific anatomy and physiology information, this study should settle the hF versus bG debate while highlighting the importance of evaluating the hemodynamic performance of a cardiac surgical

procedure, not in isolation, but in context of the global systemic circulation.

So, why is power loss differences between hF and bG not important? This can be explained by examining the SCPC junction power loss in the context of the systemic circuit. An advantage of multi-scale computational modeling is this inclusion of the patient-specific systems-level physiology on the predicted hemodynamic outcomes. Due to the fact that only a small fraction of the power loss in the pulmonary circulation actually occurs over the SCPC junction, change in the junction power loss by several folds can still only have limited effects on the overall circulation. As noted, Figure 4 illustrates the contribution of the SCPC junction power loss to the *total* pulmonary power loss in each patient. It is clear that much of the power loss via the pulmonary circulation occurs outside of the surgical junction, meaning that the patient PVR has a much larger impact on the overall physiology than the hemodynamic differences between hF and bG. We observed the same relative significance between the SCPC and total pulmonary power loss in all 6 patients. There is a caveat, however: this does not mean power loss does not matter at all. In situations or conditions where there is important lesion that impacts on blood flow, such as severe LPA stenosis or SCPC anastomotic obstruction, the power loss through a cavopulmonary connection can become high enough to be on similar order as PVR and there will be adverse hemodynamic consequences. Also, under higher metabolic states, such as exercise, as flow increases and PVR drops, the ratio between the SCPC and the total pulmonary power loss is expected to rise. Further studies will be needed to determine whether this would result in more noticeable differences in physiology between different surgical geometries.

The multi-scale simulations also revealed that in two patients with discrete left PA stenosis, virtual augmentation with arterioplasty did not lead to important benefits in the overall performance and hemodynamics of the SCPC. This suggests that, in these two patients, a more extensive and potentially risky operation (i.e. division of the Damus-Kay-Stansel anastomosis to get to the left PA) to relieve LPA stenosis would not have led to additional hemodynamic and physiologic benefits. Again, this discovery cannot be applied to all instances of left PA stenosis, as surely relief of severe left PA stenosis is important

406 at the time of a cavopulmonary connection procedure. Nonetheless, these simulation
407 results suggests that not all left PA stenosis requires extensive arterioplasty, and a
408 combination of virtual surgery with multi-scale modeling can provide valuable support and
409 guidance to a surgeon's decision on whether a patient-specific left PA stenosis can be left
410 untouched at the time of SCPC.

411 Closed loop modeling of stage 1 physiology represents a challenge due to the complexity
412 of the physiology and time-varying nature of the hemodynamic measurements. Clinical
413 data is acquired at different time points and used to build a representation of the patient's
414 pre-operative physiology. The aim of this study was to compare the effect of different
415 surgical anatomies, without additional adaptation from the global physiology.
416 Consequently, responses such as post-operative stress response, effects of medication,
417 chronic adaption to new ventricular loading conditions, post-operative complications, and
418 the effects of growth on the clinical data are not modeled. In light of this, validation of the
419 predicted results against existing clinical data remains limited. The simulations represent
420 a prediction of the *immediate* post-operative physiology based on the physiological
421 impacts of loading changes induced by the surgical procedures only. A direct comparison
422 between the surgical options is essential for gaining a mechanistic understanding of the
423 hemodynamics in the relevant clinical scenarios. One step towards assessing the
424 robustness of the predicted results would be to incorporate approaches that also contain
425 sensitivity analysis [18] or uncertainty quantification [23], including both the clinical data and
426 physiological model parameters. This might be especially important when preoperative
427 clinical data are not coherent.[13] Currently, such methods are computationally expensive
428 and in need of further development.[23] It is also important to point out that while variation
429 in the bi-directional Glenn procedure is limited, the construction of a hemi-Fontan can be
430 quite variable from one institution and one surgeon to another. As only one institution
431 (Michigan) in our collaboration routinely applied the hemi-Fontan, we have adopted virtual
432 hemi-Fontan models without additional patch enlargement of the left pulmonary artery was
433 described by William Norwood. Therefore, it is possible that an left PA stenosis will
434 routinely be addressed by this manner of hemi-Fontan construction. Finally, any virtual
435 surgery and computational modeling investigation, even using patient specific information,

cannot account for all the biological and clinical processes that impacts on ultimate outcome. Therefore, the findings from this study should be applied in the context of clinical decision-making support.

Conclusion

In this first case series of patient-specific multiscale modeling of superior cavopulmonary connection palliation for single ventricle hearts, virtual hemi-Fontan and bidirectional Glenn procedures were simulated based on each patient's *preoperative* anatomy and physiologic conditions derived from clinically indicated investigations. Despite what appeared to be significant local power loss differences, both the hemi-Fontan and bidirectional Glenn procedures resulted in similar early postoperative superior cavopulmonary hemodynamics and physiology. Moreover, simulations suggest that multi-scale modeling may be helpful to support patient-specific decision on whether an aggressive left pulmonary artery reconstruction at the time of SCPC procedure could be beneficial.

Acknowledgements and Disclosures

The authors gratefully acknowledge support from Foundation Leducq.

The authors have nothing to disclose with regard to commercial support.

References

1. Bove EL, de Leval MR, Migliavacca F, Guadagni G, Dubini G, Computational fluid dynamics in the evaluation of hemodynamic performance of cavopulmonary connections after the Norwood procedure for hypoplastic left heart syndrome. *J Thorac Cardiovasc Surg* 126, 1040-1047 (2003).

2. Pekkan K et al., Hemodynamic Performance of Stage-2 Univentricular Reconstruction: Glenn vs. Hemi-Fontan Templates. *Ann Biomed Eng* 37, 50-63 (2009).

3. Corsini C et al., An integrated approach to patient-specific predictive modeling for single ventricle heart palliation. *Comput Methods Biomech Biomed Engin*, (2013).

4. Kung E et al., Predictive modeling of the virtual Hemi-Fontan operation for second stage single ventricle palliation: Two patient-specific cases. *J Biomechanics* 46, 423-429 (2013).

5. Schiavazzi DE et al., Hemodynamic effects of left pulmonary artery stenosis after superior cavopulmonary connection: A patient-specific multiscale modeling study. *J Thorac Cardiovasc Surg* 149, 689-696.e683 (2015).

6. Vignon-Clementel IE, Marsden AL, Feinstein JA. A primer on computational simulation in congenital heart disease for the clinician. Prog. Pediatr. Cardiol. 30(1), 3–13, 2010.

7. Corsini C et al., An integrated approach to patient-specific predictive modeling for single ventricle heart palliation. *Comput Methods Biomech Biomed Engin,* (2013).

8. Schievano S et al., Percutaneous pulmonary valve implantation based on rapid prototyping of right ventricular outflow tract and pulmonary trunk from MR data. *Radiology* 242, 490-497 (2007).

9. Snyder MF, Rideout VC, 1969. Computer simulation studies of the venous circulation. *IEEE Transactions on Biomedical Engineering* 16, 325–334.

10. Noordergraaf A, Verdouw D, Boom HB, 1963. The use of an analog computer in a circulation model. *Progress in Cardiovascular Diseases* 5, 419–439.

11. Pennati G, Fumero R, 2000. Scaling approach to study the changes through the gestation of human fetal cardiac and circulatory behaviors. *Annals of Biomedical Engineering* 28, 442–452.

12. Kung E et al., Predictive modeling of the virtual Hemi-Fontan operation for second stage single ventricle palliation: Two patient-specific cases. *J Biomech* 46, 423-429 (2013).

13. Arbia, G., Corsini, C., Baker, C., Pennati, G., Hsia, T.-Y., Vignon-Clementel, I., 2015. Pulmonary hemodynamics simulations before stage 2 single ventricle surgery: Patient-specfic parameter identification and clinical data assessment. *Cardiovascular Engineering and Technology*, 1-13.

14. Brody JS, Stemmler EJ, DuBois AB. Longitudinal distribution of vascular resistance in the pulmonary arteries, capillaries, and veins. *J. Clin. Invest.* 47, 783–799 (1968). DOI 10.1172/JCI105773

15. O'Leary CE, Fiori R, Hakim TS. Perioperative distribution of pulmonary vascular resistance in patients undergoing coronary artery surgery. *Anesth. Analg.* 82, 958–963 (1996)

16. Presson RG, Audi SH, Hanger CC, Zenk GM, Sidner RA, Linehan JH, Wagner WW, Dawson CA. Anatomic distribution of pulmonary vascular compliance. *J. Appl. Physiol.* 84, 303–310 (1998)

17. Spilker RL, Feinstein JA, Parker DW, Reddy VM, Taylor CA, 2007. Morphometry-based impedance boundary conditions for patient-specific modeling of blood flow in pulmonary arteries. *Annals of Biomedical Engineering* 35, 546–559.

18. Troianovski G., Taylor CA, Feinstein JA, Vignon-Clementel IE. 2011. Three-dimensional simulations in Glenn patients: clinically based boundary conditions, hemodynamic results and sensitivity to input data. *Journal of Biomechanical Engineering* 133, 111006.

19. Baker CE et al., Effects of pulmonary artery banding and retrograde aortic arch obstruction on the hybrid palliation of hypoplastic left heart syndrome. *J Thorac Cardiovasc Surg,* (2013).

20. Hsia TY et al., Use of mathematical modeling to compare and predict hemodynamic effects between hybrid and surgical Norwood palliations for hypoplastic left heart syndrome. *Circulation* 124, S204-210 (2011).

21. Esmaily Moghadam M., Bazilevs Y, Hsia TY, Vignon-Clementel IE, Marsden AL, A comparison of outlet boundary treatments for prevention of backflow divergence with relevance to blood flow simulations. *Computational Mechanics*, 1-15 (2011).

22. Dasi, L. P., KrishnankuttyRema, R., Kitajima, et al.. Fontan hemodynamics: importance of pulmonary artery diameter. *J Thoracic Cardiovasc Surg*, 137(3), 560-

564. (2009)

23. Schiavazzi DE, Arbia G, Baker C, Hlavacek AM, Hsia TY, Marsden AL, Vignon-Clementel IE, et al. Uncertainty quantification in virtual surgery hemodynamics predictions for single ventricle palliation. *International Journal for Numerical Methods in Biomedical Engineering*, 2015.

24. de Leval MR, Dubini G, Migliavacca F, Jalali H, Camporini G, Redington A, Pietrabissa R. Use of computational fluid dynamics in the design of surgical procedures: application to the study of competitive flows in cavo-pulmonary connections. J Thorac Cardiovasc Surg. 1996 Mar;111(3):502-13.

536

537

538 **List of Tables**

Table 1: Pre-operative demographics of the six patients used for the study

Patient	**A**	**B**	**C**	**D**	**E**	**F**
Age* (months)	6	3	4	3	4	5
BSA (m^2)	0.34	0.30	0.27	0.26	0.28	0.34
Diagnosis	PA/IVS	MS, AS	MS, AS	TA, PA left PAS	MA, AA	MA, AA
Stage 1 surgery	3.5mm mBTS	Norwood 3.5mm mBTS	Norwood 3.5mm mBTS	4mm mBTS with LPAplasty	Norwood 3.5mm mBTS	Norwood 3.5mm mBTS

*Age used for model construction

BSA: body surface area; PA/IVS: pulmonary atresia/intact ventricular septum; mBTS: modified Blalock-Taussig shunt; MS: mitral stenosis; AS: aortic stenosis; TA: tricuspid atresia, PAS: pulmonary artery stenosis; MA: mitral atresia; AA: aortic atresia

Table 2: Clinical parameters used for pre-operative multiscale modeling

Patient	A	B	C	D	E	F
CI ($L/min/m^2$)	4.31	4.08	6.87	6.23	5.79	5.47
Qp ($L/min/m^2$)	1.32	1.94	3.69	2.77	2.57	3.53
Qrpa : Qp (%)	64	46	51	67	46	55
Qp : Qs	0.44	0.91	1.16	0.80	0.80	1.81
mP_{atr} (mmHg)	5	6	6	7	5	4
mPAP (mmHg)	13(R), 12(L)	12(R/L)	11(L)	17(R), 14(L)	13 (L)	13.5(L)
TPG (mmHg)	8	6	5	10	8	9.5
mP_{Ao} (mmHg)	43[#]	52	51	53	53	72
PVR ($WU*m^2$)	6.0	3.1	1.4	3.6	2.8	2.7
SVR ($WU*m^2$)	12.7	21.5	14.2	13.3	14.8	35.0

[#]estimated from left upper limb sphygmomanometer

CI: cardiac index; Qp and Qs: pulmonary and systemic flow; Qrpa: right pulmonary artery flow; mP_{atr} : mean systemic atrial pressure; mPAP: mean pulmonary artery pressure; R/L: right/left; TPG: transpulmonary gradient; mP_{Ao}: mean invasive ascending aortic pressure; PVR and SVR: pulmonary and systemic vascular resistance.

Table 3: SCPC simulation results

Patient	A		B				C		D				E		F	
Procedure	**bG**	**hF***	**bG**	**bG(ns)***	**hF**	**hF(ns)**	**bG***	**hF**	**bG**	**bG(ns)***	**hF**	**hF (ns)**	**bG**	**hF***	**bG**	**hF***
CI (L/min/m^2)	3.40	3.38	3.34	3.35	3.34	3.35	5.25	5.24	4.29	4.32	4.28	4.32	3.87	3.86	3.64	3.64
Qp (L/min/m^2)	2.01	1.99	1.63	1.64	1.63	1.64	2.88	2.87	2.66	2.70	2.65	2.69	2.74	2.73	2.58	2.58
Qrpa : Qp (%)	63	63	59	54	59	54	51	48	69	61	68	60	45.0	45.0	56	55
Qp : Qs	0.59	0.59	0.49	0.49	0.49	0.49	0.55	0.55	0.62	0.62	0.62	0.62	0.71	0.71	0.71	0.71
P_atr (mmHg)	2.48	2.43	4.59	4.62	4.60	4.63	5.22	5.22	4.67	4.71	4.66	4.71	3.63	3.62	2.46	2.46
Psvc (mmHg)	15.07	15.38	10.49	10.02	10.43	10.02	10.11	10.19	14.67	13.76	14.91	13.84	11.92	12.09	10.30	10.26
TPG (mmHg)	12.18	12.13	5.05	4.70	5.07	4.93	4.25	4.24	8.05	8.34	8.04	8.37	8.19	8.18	7.20	7.20
Ao MAP (mmHg)	53.06	53.10	74.9	74.9	74.9	74.9	80.4	80.42	67.0	66.9	67.1	66.9	65.9	65.9	131.4	131.4
3D Power loss (mW)	0.61	1.26	0.87	0.35	0.82	0.33	1.05	1.24	2.00	0.92	2.51	1.11	0.95	1.28	1.20	1.12
PA-Sa power loss (mW)	18.49	18.18	5.54	5.59	5.57	5.62	15.54	15.61	13.31	13.15	13.14	13.08	13.81	13.74	14.00	13.98
Total pulmonary power loss	19.10	19.44	6.41	5.94	6.39	5.95	16.59	16.85	15.31	14.07	15.65	14.19	14.76	15.02	15.20	15.10
SCPC : Total Pulmonary power loss (%)	3.2	6.5	13.6	5.9	12.8	5.5	6.3	7.4	13.1	6.5	16.0	7.8	6.4	8.5	7.9	7.4
Oxygen delivery (mlO_2/min/m^2)	597	593	599	602	602	603	1006	1005	806	812	804	812	746	746	867	867
O_2 sat Ao	82	82	84	84	84	84	89	89	88	88	88	88	90	90	91	91

*actual surgical procedure performed

SCPC: superior cavopulmonary connection; bG: bidirectional Glenn; hF: hemi-Fontan; ns: no left PA stenosis; CI: cardiac index; Qp and Qs: pulmonary and systemic flow; Qrpa: right pulmonary artery flow; P_atr: common atrial pressure; Psvc: superior vena cava pressure; TPG: transpulmonary gradient; Ao MAP: aortic mean arterial pressure; PA-Sa: pulmonary artery to systemic atrial; Ao: a

Figure Legends

Figure 1. An example of the virtual bG and hF superior cavopulmonary surgeries using patient B. Top panel demonstrates the preoperative (Stage 1) anatomy obtained from MRI. Middle panel demonstrates virtual bG and hF surgeries. Bottom panel demonstrates virtual bG and hG procedures with concomitant left pulmonary arterioplasty for relieve of left pulmonary arterial stenosis. SVC: superior vena cava; BTS: Blalock-Taussig shunt; atr: atrium; bG: di-directional Glenn; hF: hemi-Fontan; PA: pulmonary artery

Figure 2. The preoperative anatomical reconstruction (stage 1) and virtual surgery (stage 2) for all six patients studied. Patients B and D had left pulmonary arterial stenosis preoperatively, and virtual SCPC surgeries were performed with and without concomitant left pulmonary arterioplasty. bG: di-directional Glenn; hF: hemi-Fontan; PA: pulmonary artery

Figure 3: Mid-systolic pressure and velocity maps for patient B. Panel A: bi-directional Glenn with left pulmonary artery stenosis; panel B: hemi-Fontan with left pulmonary artery stenosis; panel C: bi-directional Glenn with pulmonary arterioplasty; panel D: hemi-Fontan with pulmonary arterioplasty.

Figure 4. A comparison of the power loss in the SCPC surgical junction and the total power loss through the pulmonary circulation. Power loss through the SCPC surgical junction, whether bG or hF, represents a very small part of the overall power loss in the superior cavopulmonary circulation. bG: di-directional Glenn; hF: hemi-Fontan; PA: pulmonary artery; ns: no pulmonary arterial stenosis; mW: milli-Watts.

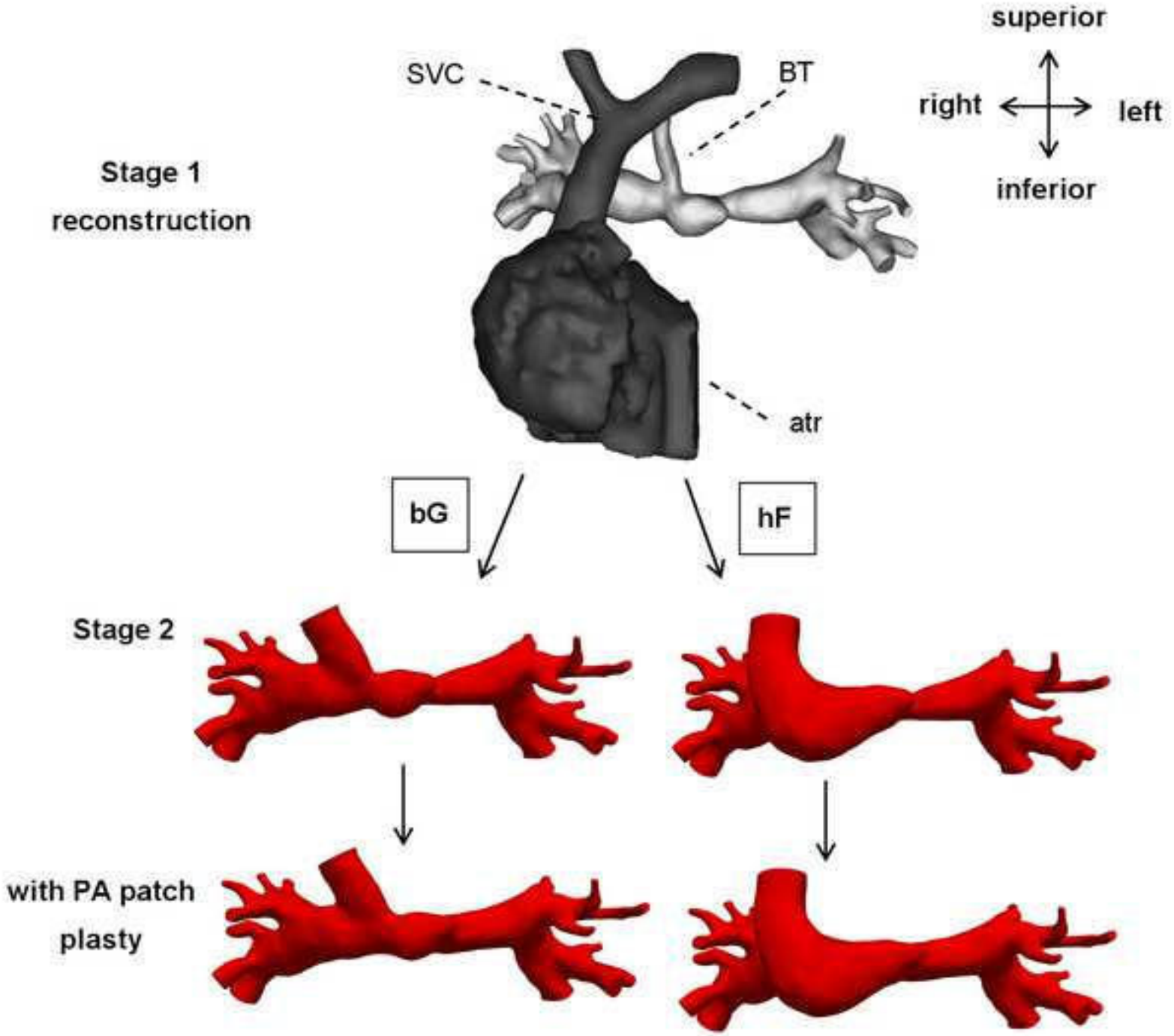

Figure

Click here to download Figure Fig2_finalR1.tiff

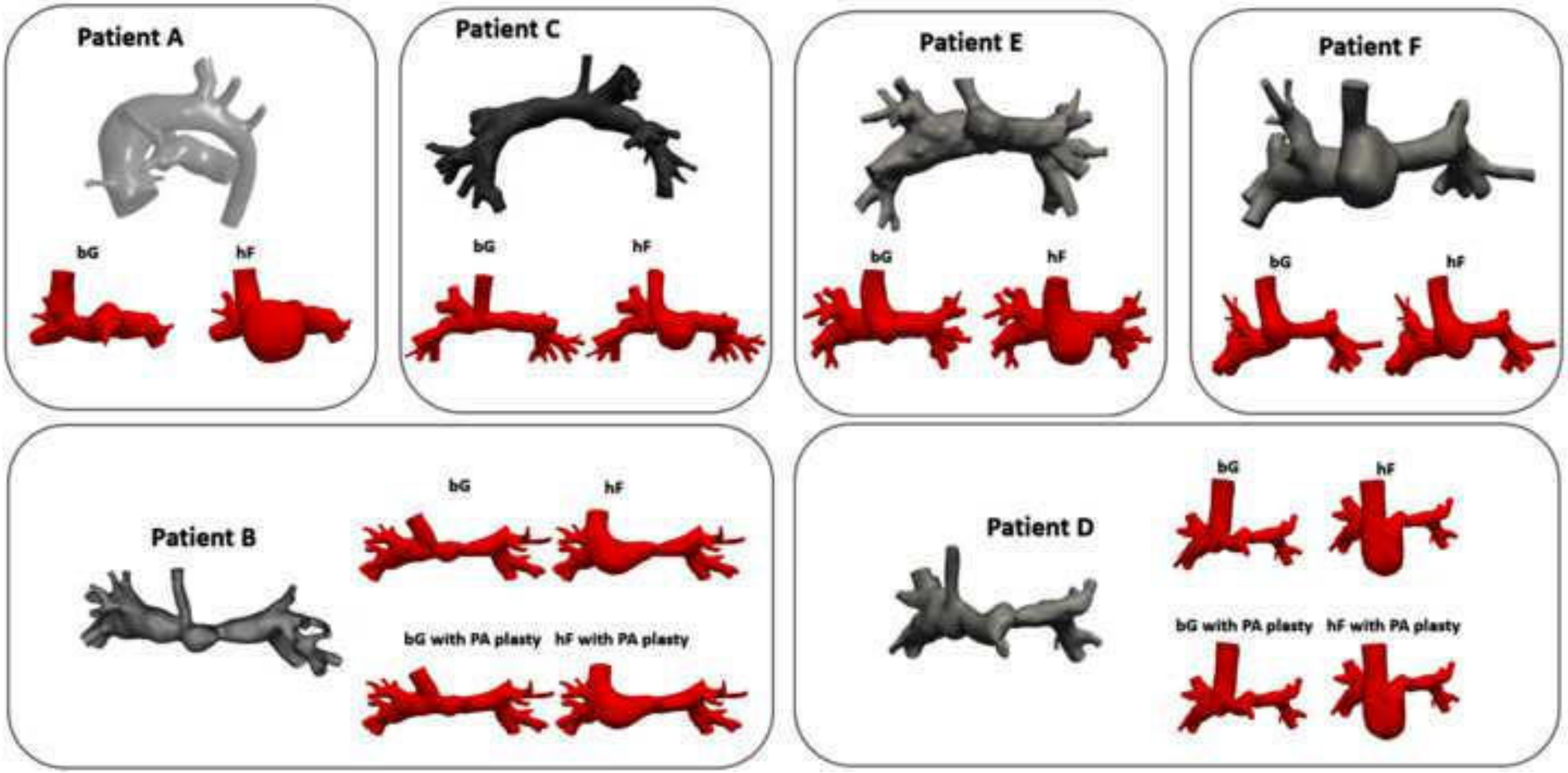

Figure

Click here to download Figure fig3R1.tif

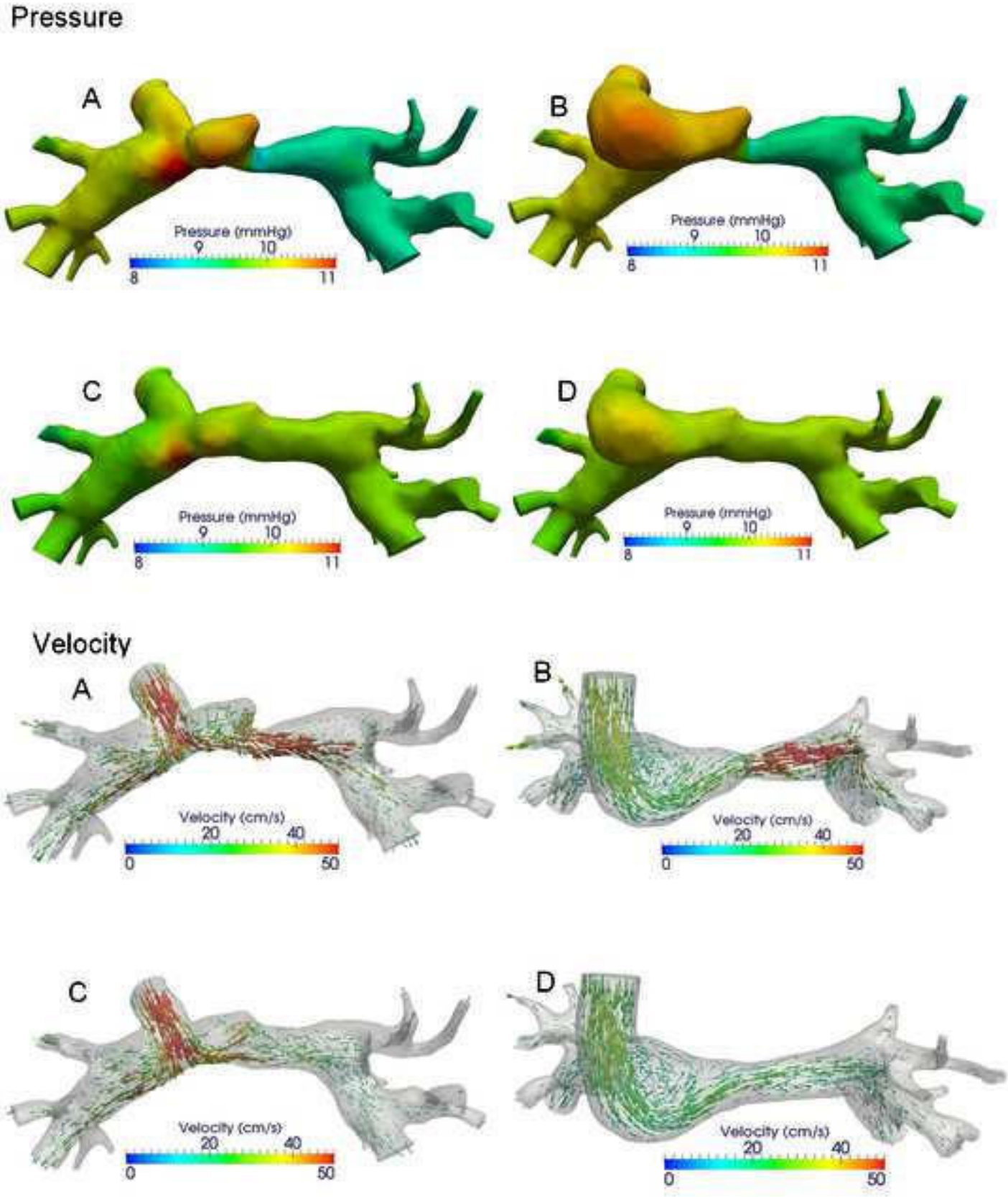

Figure

Click here to download Figure fig4R1.tif